



# Heavy Metal Removal from Aqueous Solutions Using Fly-Ash Derived Zeolite NaP1

Archibald Frank Ankrah<sup>1</sup> · Begum Tokay<sup>1</sup> · Colin E. Snape<sup>2</sup>

Received: 30 September 2021 / Revised: 5 January 2022 / Accepted: 8 February 2022  
© The Author(s) 2022

## Abstract

Fly-ash derived zeolites have recently received great attention as cheaper adsorbents to remove heavy metals from water since they can be synthesized from a waste product. In this study, we evaluated the single- and multi-cation adsorption efficiencies of fly-ash derived NaP1 for the removal of zinc (Zn), copper (Cu) and lead (Pb). We also determined precipitation and leaching from NaP1 during the adsorption. Results showed that the uptake capacities for Zn (34 mg/g) and Pb (192 mg/g) were higher than other fly-ash derived NaP1 and adsorbents such as clinoptilolite and activated carbon. The Cu uptake was estimated ~ 14.6 mg/g.  $Pb^{2+} > Cu^{2+} > Zn^{2+}$  is the order for the metal cation selectivity of NaP1. Langmuir adsorption isotherm and pseudo-second order kinetic model fitted best for all elements. The metal uptake occurred in 15 min. Diffusion of hydrated metals through microporous channels is the rate-determining step.

## Article Highlights

- Fly-ash derived NaP1 adsorbed 34.2 mg g<sup>-1</sup> Zn<sup>2+</sup>, 14.6 mg g<sup>-1</sup> Cu<sup>2+</sup> and 192 mg g<sup>-1</sup> Pb<sup>2+</sup>.
- Ion selectivity of NaP1 is in the order of  $Pb^{2+} > Cu^{2+} > Zn^{2+}$ .
- Langmuir and pseudo-second order kinetic models fitted best for all elements.
- The metal uptake occurred in 15 min for both single and multi-element adsorption.
- Leaching and precipitation were evaluated.

**Keywords** Fly-ash derived zeolites · Heavy-metal removal · Ion selectivity · Multi-cation adsorption · NaP1

## Introduction

Accelerated industrialisation and population growth in developing countries has generated vast quantities of wastewater effluents, comprising of wide variety of heavy metal ions into environment within the past decades. Direct disposal of these wastewater will impose serious threat to the environment and have lethal effects on the community due to their toxicity and carcinogenic nature (Timothy

and Williams 2019). Industries such as electroplating, mines, pharmaceuticals, paint and textile, are the major point source, producing effluents constitute heavy metals (Tchounwou et al. 2012; Bazrafshan et al. 2015) such as zinc, lead, copper, nickel and cadmium, regardless of the economic benefits that these industries offer to the communities. Hence, there is a requirement to explore eco-friendly (Tokay and Akpınar 2021), sustainable, cost effective and efficient adsorbents while eliminating pollution (Klučáková and Pavlíková 2017).

Various heavy metal removal technologies have been explored to date. Adsorption is preferred to others such as reverse osmosis (Quadis and Moussa 2004), electrocoagulation (Bazrafshah et al. 2015), ultrafiltration (Cao et al. 2020), filtration (Abdullah et al. 2019), coagulation and precipitation (Charerntanyarak 1999). The process is economically viable, highly efficient, easy to be operated and possesses great availability of adsorbent compared to other techniques.

✉ Begum Tokay  
begum.tokay@nottingham.ac.uk

<sup>1</sup> Department of Chemical and Environmental Engineering, Faculty of Engineering, University of Nottingham, University Park, Nottingham NG7 2RD, UK

<sup>2</sup> Energy Technologies Building, Faculty of Engineering, University of Nottingham, Jubilee Campus, Nottingham NG8 1BB, UK

Designing and operation stage of adsorption processes are flexible, and the process can produce high-purity effluent (Perić et al. 2004; Asim et al. 2020). At present, the most widely applied porous adsorbents include activated carbon, carbon nanotubes, zeolite, clay minerals, biosorbent and biopolymers. However, most of these commercial adsorbents have become more expensive due to the increasing demand, high cost of production and regeneration (Zwain et al. 2014; Kołodziej et al. 2017; Erdem et al. 2004). Therefore, alternative adsorbents are crucial.

Zeolites are well known for their extensive ion exchange and adsorption capabilities (Margeta et al. 2013). Existing as both natural and synthetic, they have been used in petroleum refinery, water softening, heavy metal removal, separation of gases, dehumidifiers and many more applications (Li et al. 2019). Synthetic zeolites have been preferred over natural zeolites due to their tailorable properties, higher purity and high thermal stability (Li et al. 2019). However, synthetic zeolites are also becoming more expensive due to increasing demand, requiring cheaper precursors to promote sustainability.

Fly-ash from coal combustion power plants contains high amounts of quartz and mullite, composed of necessary precursors for the synthesis of zeolites (Yan et al. 2018). Thus, recycling waste from coal fly-ash to remove pollutants from water is a possible low-cost method for preparing synthetic zeolites, reinforcing sustainability, waste recycle, and thus industrial symbiosis. Fly-ash has mostly been used as construction material production (Ramesh et al. 2020), representing about 48% of the total amount, while most of the fly-ash was landfilled (Brännvall and Kumpiene 2016). To date, zeolite X, A, chabazite, sodalite and NaP1 have been synthesised from fly ash. Zeolite X and A are in high demand due to their uniform pore structure and larger pore size, compared to NaP1 (Alvarez-Ayuso et al. 2003), sodalite and chabazite. However, fly-ash derived zeolites X and A are more expensive to synthesize, compared to NaP1, through the conventional hydrothermal synthesis process as they require large quantities of raw materials (aluminates, silicon and NaOH) and a 2-step process (Czuma et al. 2019). Fly-ash derived NaP1 can be produced with a high yield (45–75%), compared to fly-ash derived zeolites X and A (16–18%) in a one-step process using low amount of raw materials (Moreno et al. 2001; Querol et al. 2001). Thus, fly-ash derived NaP1 is preferable due to its high yield, cost and duration of production and ease of preparation.

NaP1 has been tested for removal of heavy metals such as Zn, Cu, Ni and Cd in acid mine (Prasad and Mortimer 2011), electroplating wastewater (Steenbruggen and Hollman 1998; Alvarez-Ayuso et al. 2003) and synthetic water matrix (Lee et al. 2000; Nascimento et al. 2009). Lee et al. (2000) explored synthetic fly-ash derived NaP1 for zinc, copper and lead removal from water matrix of concentration

(20–400 mg/l) using 0.1 g zeolite in a litre of solution at 25 °C. Although there is no record of pH adjustment and contact time. They reported 65.8 mg/g, 73.5 mg/g and 267 mg/g adsorptive capacities for zinc, copper and lead, respectively. Similarly, Moreno et al. (2001), Querol et al. (2002) and Prasad and Mortimer (2011) tested synthetic NaP1 on zinc removal from acid mine wastewater with initial concentrations of 65 mg/l, 54 mg/l and 174 mg/l, respectively. Contact time for all experiments was reported as 1 h with initial pH values of > 4.6, 5.5 and 2.5–5.5, respectively, without further pH adjustment during the experiment. These experiments showed more than 94% removal efficiency for NaP1. Alvarez-Ayuso et al. (2003) treated zinc and copper from an electroplating wastewater finishing effluent (125 mg/l) at pH 6 in 1 h using 2.5 mg/l adsorbent. They obtained an adsorptive capacity of 32.6 and 50.5 mg/g for zinc and copper, respectively. Nascimento et al. (2009) tested NaP1 for lead, zinc and copper removal from water and reported adsorptive capacities of 195 mg/g, 59.2 mg/g and 76.9 mg/g, respectively. They conducted their experiments at pH of 4–5, with the metal concentrations in the range of 100–3000 mg/l using 10 g/l adsorbents over 2 h at 25 °C. These studies have limited scope since the removal conditions (i.e., pH, temperature and concentrations of metals) considered were either narrow to a localized wastewater (target specific) or not relevant to industrial conditions. In addition, they did not report on leaching or precipitation. Moreover, current research on NaP1 does not present a clear distinction of the heavy metal removal mechanism (i.e., ion exchange, adsorption and precipitation) at relevant industrial conditions, providing limited information to adopt NaP1 for industrial applications.

In this study, we evaluated the use of fly-ash derived zeolite NaP1 for the remediation of copper, zinc and lead from water, mimicking electroplating plant effluent. Adsorption selectivity, kinetics and adsorptive capacity of NaP1 were determined via single and multi-cation batch adsorption experiments. For the first time, we evaluated the precipitation and leaching from the adsorbent for a wide range of conditions. Various techniques including X-ray diffraction, scanning electron microscopy and X-ray fluorescence spectroscopy were used to characterise the samples.

## Experimental

### Materials

Zeolite NaP1 was provided by Lublin University of Technology, Poland, synthesized from class F fly-ash, obtained from a Polish coal power plant. Wdowin et al. (2014) described the method used to synthesise zeolites from fly-ash as one of the precursors. NaP1 is the synthetic form of

the gismondine-type zeolite. The crystal structure is made up of 2-dimensional pore system 8-member oxygen ringed channels (0.31 × 0.44 nm) and (0.26 × 0.49 nm) in the (100) and (010) direction, respectively, connected by a double crankshaft chain made up of four rings (Sharma et al. 2016). The effective pore size of NaP1 is ~0.29 nm (Alvarez-Ayuso et al. 2003).

Copper nitrate (Cu(NO<sub>3</sub>)<sub>2</sub>·3H<sub>2</sub>O, 98%), zinc nitrate (Zn(NO<sub>3</sub>)<sub>2</sub>·6H<sub>2</sub>O, 98%), lead nitrate (Pb(NO<sub>3</sub>)<sub>2</sub>, 98%), sodium hydroxide pellets (NaOH, 99.9%), nitric acid (HNO<sub>3</sub>, 68%), hydrochloric acid (HCl, 37%) and ammonium acetate (NH<sub>4</sub>COOH, 98%) were purchased from Fisher Scientific.

## Characterisation

Bruker D8 Advance X-ray diffractometer (XRD) was used to characterize the powder samples. Samples were measured with a 0.6 slit for 2 h at 25 ± 2 °C and scanned between 5° and -65° 2θ with increments of 0.05° in 2 s. Cu Kα radiation was used at 40 kV and 35 mA.

The qualitative and quantitative elemental composition of the zeolite samples were determined using a Panalytical Epsilon 3XL X-ray fluorescence analyser (XRF) before and after adsorption. Powder samples (~5 g) were ground, placed in a plastic cup (approx. 4.9 cm in depth) and covered with a plastic film at the bottom.

Philips XL30 scanning electron microscope, operated at 15 kV, was used to evaluate the shape and size of the NaP1 crystals. NaP1 crystals were sprinkled on sample stubs with carbon adhesives. Before use, crystals were carbon coated using Edwards E306A film coater (10 nm thin layer, high vacuum, 30 V/30 A).

The nitrogen adsorption/desorption isotherms were obtained using a Micromeritics ASAP 2420 V2.09. Samples were degassed in the chamber (at 250 °C) to remove any adsorbed gases and water prior to experiments. The pore size and the volume and BET surface area were reported.

## Adsorption Experiments

For single metal cation adsorption experiments, Pb, Cu and Zn concentrations were set to 100, 150 and 250 mg/l, respectively, in purified water (at 18.2 MΩ.cm resistivity). The pH (Jenway 570 with temperature correction function) of the solutions was maintained at a range of 3–4 using 68% HNO<sub>3</sub> and 2% wt/v NaOH solutions to prevent precipitation of Cu ions. Approximately 5 g/l zeolite samples were used during the experiments. The solutions were mixed on a magnetic stirrer up to 3 h at 22 ± 2 °C. Preliminary multi-cation adsorption experiments were conducted using 1 g/l NaP1 at pH 3.5, 20 ± 2 °C with the same initial heavy metal concentrations (12.5 mg/l) for all heavy metals to eliminate the concentration effect.

For the determination of the adsorption isotherms, the concentrations of individual heavy metal solutions were adjusted in the range of 50–1000 mg/l, 50–3500 mg/l and 50–2800 mg/l for Cu, Zn and Pb, respectively. The pH, temperature and amount of adsorbent were the same as the multi-cation adsorption experiments. All experiments were repeated two times to observe errors associated. The sampling amount was not exceeded 5–10% of the solution amount.

The adsorption kinetics during the adsorption of heavy metal ions was determined by employing the pseudo-first (Eq. 1) and -second order (Eq. 2) kinetic models as follows:

$$\ln(Q_e - Q_t) = \ln(Q_e) - k_1 \times t, \quad (1)$$

$$\frac{t}{Q_t} = \frac{1}{k_2 \times Q_e^2} + \frac{1}{Q_e}, \quad (2)$$

where  $Q_t$  (mg/g) and  $Q_e$  (mg/g) are the adsorbed amount of metal ions at time  $t$  (min) and at equilibrium, respectively.  $k_1$  (1/min) and  $k_2$  (g/mg min) are the pseudo-first and -second order rate constants, respectively.  $t$  (min) represents the adsorption time.

Freundlich (Eq. 3) and Langmuir (Eq. 4) models were employed to determine the adsorption mechanism and the maximum adsorption capacity at equilibrium as follows:

$$Q_e = K_F \cdot C_e^{\frac{1}{n}}, \quad (3)$$

where  $K_F$  is the Freundlich isotherm constant, indicating the adsorption capacity of the adsorbent.  $C_e$  represents the adsorbate concentration in the solution at equilibrium and  $1/n$  indicates the adsorption intensity between the NaP1 and metal ions.

$$\frac{C_e}{q_e} = \left( \frac{1}{bq_m} \right) + \frac{C_e}{q_m}, \quad (4)$$

where  $q_e$  is the amount of solute adsorbed per unit mass of adsorbent.  $b$  (l/mg) is Langmuir constant.  $C_e$  represents the adsorbate concentration in the solution while  $q_m$  shows the maximum adsorption capacity of the adsorbent at equilibrium, estimated by the linear Langmuir adsorption model.

Zeolite NaP1 was also tested for leachates under the same adsorption conditions (pH 3.5,  $T = 22 \pm 2$  °C, 5 g/l NaP1) to determine the release of the elements into the purified water, in the absence of heavy metal ions. The experiments were repeated three times.

The effect of precipitation was quantified and deducted from the resulting metal uptake experiments. Precipitations of Cu, Zn, Pb were determined at pH 3.5, without zeolite, at 20 ± 2 °C. Initial Cu<sup>2+</sup>, Zn<sup>2+</sup> and Pb<sup>2+</sup> concentrations were set to approx. 12.5 mg/l for each element.

Sampling (12 ml) was conducted from the solutions at predetermined times for analyses using inductively coupled plasma atomic emission spectroscopy (ICP-AES, Perkin Elmer 300 DV). The NaP1 was separated from solutions using a centrifuge (Hettich, Rotofix 32 A) at 4000 rpm for 8 min. The supernatant was decanted and filtered (Minisart® 0.2 µm, hydrophilic). Ten ml from the filtered solution was then pipetted in a 15-ml polypropylene conical tube, acidified with 5 ml of 30% (v/v) nitric acid and refrigerated to prevent metal precipitation and microbial degradation. Calibration standards were prepared using a multi-cation solution. Purified water was also tested in every batch.

## Results and Discussions

### Characterization

The XRD pattern of zeolite NaP1 confirmed the presence of NaP1 structure, represented by the characteristic peaks at 12.5°, 17.8°, 21.6°, 28.2°, 31°, 33.4° and 46° 2θ (Supplementary Information, (SI) Fig S1). The XRD pattern also shows the peaks of mullite and quartz.

The SEM image of NaP1 shows the agglomeration of cubes (min 0.2 micron) into larger particles in the size range of 4.5–6 µm, forming a rough heterogeneous surface (Fig. S2). Wdowin et al. (2014) described this appearance as lamellar aggregates of plate-like shapes as a characteristic feature of NaP1.

The chemical composition of zeolite NaP1 synthesized from coal fly-ash is presented in Table 1. Quantitative analysis using XRF showed that most of the zeolite constitutes SiO<sub>2</sub>, Al<sub>2</sub>O<sub>3</sub> and Na<sub>2</sub>O, as expected. In addition, oxides of Mg, Ca and Fe accounted for ~7–8% of the remaining composition.

Silicon dioxide to aluminium oxide (SiO<sub>2</sub>/Al<sub>2</sub>O<sub>3</sub>) ratio for NaP1 was estimated as 1.51. The SiO<sub>2</sub>/Al<sub>2</sub>O<sub>3</sub> ratio was used as an indicator of sorption properties (Ouki and Kavannah 1997). Ramesh and Reddy (2011) reported that zeolites with Si/Al ratio between 1.0 and 1.5 represents the potential of higher sorption and ion exchange capability. This is due to

**Table 1** Percentage composition of zeolite NaP1 obtained from XRF using 5 g sample

Compounds	Percentage (%) in NaP1
Na <sub>2</sub> O	17.2
MgO	0.7
Al <sub>2</sub> O <sub>3</sub>	29.0
SiO <sub>2</sub>	43.8
CaO	2.9
Fe <sub>2</sub> O <sub>3</sub>	3.9
Other metals	2.5

the exchange of aluminium ions with silicon ions, providing a negative framework for that zeolite.

Nitrogen adsorption/desorption isotherms observed follow Type II IUPAC classification with an H3 hysteresis loop (Fig. 1). This is characteristic of a mesoporous material of pore size between 2 and 50 nm. The Type II isotherm (adsorption) indicates monolayer–multilayer adsorption while the H3 hysteresis loop (desorption) represents plate-like particles, forming slit-shaped pores. BET area and pore diameter were estimated as ~60 ± 0.1 m<sup>2</sup>/g and 11 ± 0.1 nm, respectively.

The isotherms below  $P/P_o < 0.05$  shows the presence of micropores, whereas the  $P/P_o > 0.06$  demonstrates larger pores filled at higher pressure. The  $0.01 < P/P_o < 0.06$  region of the plot is also known as the knee, which shows the end of monolayer adsorption coverage of adsorbent surface. The micropore region of the isotherm indicates that the low-pressure uptake of nitrogen gas is limited. For  $0.06 < P/P_o < 0.45$  region, where larger pores are accessed, multilayer adsorption starts and thus the volume of nitrogen adsorbed was increased with increasing relative pressure. Capillary condensation, which was observed during the desorption, suggests the presence of mesopore structure that is also confirmed by the pore size diameter.

### Leaching and Precipitation

Leaching tests from NaP1 was undertaken at the adsorption conditions (3 h, pH = 3.5 and  $T = 20 \pm 2$  °C) in the presence of zeolite (5 g/l) without heavy metals (Table S1, S2). The leaching experiments showed that, Cu<sup>2+</sup> (13.6 µg/g), Zn<sup>2+</sup> (61 µg/g) and Pb<sup>2+</sup> (6 µg/g) ions leached into water from NaP1 only at microgram levels in the first 15 min and concentrations were constant until 60 min. These concentrations are below the allowed effluent discharge limits and thus negligible compared to initial heavy metal concentrations

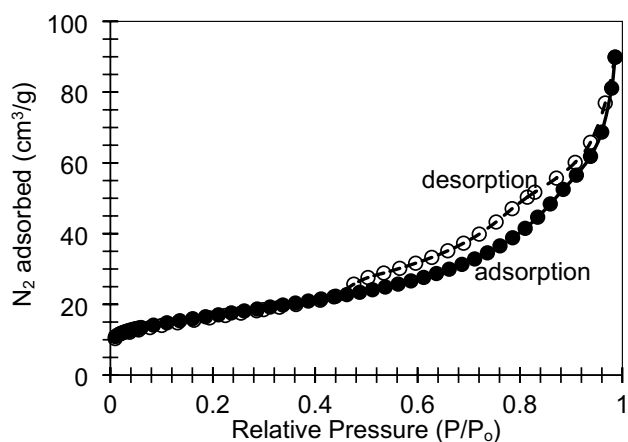


**Fig. 1** Nitrogen adsorption–desorption isotherms for NaP1

in the water. Similarly,  $\text{Na}^+$ , (23 mg/g),  $\text{Ca}^{2+}$  (11.4 mg/g),  $\text{K}^+$  (2.8 mg/g) and  $\text{Al}^+$  (21.2 mg/g) released into water within the first 15 min and stayed at similar levels until 60 min. These leachates are negligible when the content of NaP1 compared with Table 1. Therefore, leaching from NaP1 is not considered as a problem during the adsorption experiments.

The effect of precipitation was quantified and deduced from the resulting adsorption experiments, where needed. Table 2 shows the heavy metal precipitation at pH (3.5, 6.5, 10.5) from control experiments when 1 L water matrix was stirred for 1 h without zeolite.

The highest percentage of precipitation for all the heavy metals (> 95%) was observed at pH 10.5 due to the formation of metal hydroxides of copper, zinc and lead. These metal hydroxides are not soluble in water above the pH values of 5.3, 7.5 and 6, for Cu, Zn and Pb, respectively (Marchioretto et al. 2005). Therefore, the lowest heavy metal precipitation (3%) was observed at pH 3.5, conforming the absence of precipitation. Copper (2.61 mg/l) and lead (2.89 mg/l) precipitated, representing approximately 23% of the starting concentration at pH 6.5. Zinc precipitation (1.2 mg/l) was lower than copper and lead and equals to 9.2% of the starting concentration at pH 3.5. Copper and lead hydroxide formation/precipitation begin from pH > 5.3 and pH > 6, respectively, while zinc hydroxide formation begins pH > 7.5. This explains the low zinc precipitation that was observed at pH 6.5.

### Adsorption Experiments

Figure 2 shows the single cation adsorption and control experiments (without zeolite), conducted using NaP1 at pH 3.5. A steep decline in concentrations were observed within the first 15 min for all metals, followed by a slight decrease until 60 min. This trend indicates that most of the adsorption sites available were occupied in 15 min, followed by a slow diffusion of metal ions through the pores of zeolite NaP1 until further saturation was achieved (Motsi et al. 2009) Zinc, lead and copper concentrations were measured as 217, 4.11 and 115 mg/l at the end of the adsorption experiments.

**Table 2** Concentrations of heavy metal cations in water as a function of time at pH 3.5, 6.5 and 10.5 ( $T=20\pm 2\text{ }^\circ\text{C}$ , no zeolite, 1 h)

pH	Time (h)	$\text{Cu}^{2+}$ (mg/l)	$\text{Zn}^{2+}$ (mg/l)	$\text{Pb}^{2+}$ (mg/l)
3.5	0	$11.4\pm 0.1$	$13.1\pm 0.1$	$12.4\pm 0.13$
	1	$11.2\pm 0.12$	$13.0\pm 0.11$	$12.3\pm 0.1$
6.5	0	$11.4\pm 0.1$	$13.1\pm 0.12$	$12.4\pm 0.03$
	1	$8.8\pm 0.1$	$11.9\pm 0.1$	$9.5\pm 0.14$
10.5	0	$11.4\pm 0.1$	$13.1\pm 0.1$	$12.4\pm 0.1$
	1	$0.0045\pm 0.003$	$0.053\pm 0.004$	$0.55\pm 0.01$

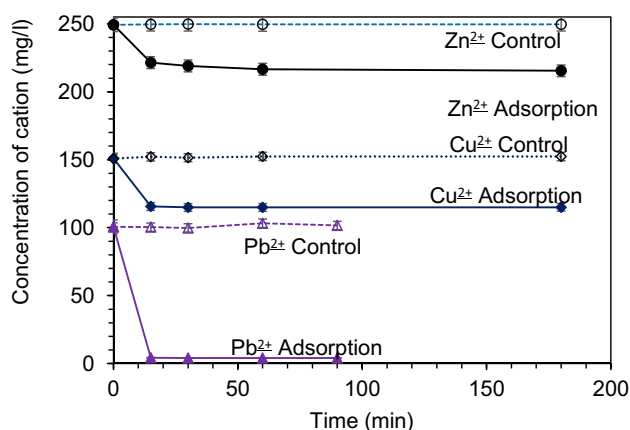


**Fig. 2** Concentrations of cations in water during single cation adsorption (1 g/l NaP1) and precipitation/control experiments (without zeolite) as a function of time. Conditions:  $\text{Zn}^{2+}=250\text{ mg/l}$ ,  $\text{Cu}^{2+}=150\text{ mg/l}$ ,  $\text{Pb}^{2+}=100\text{ mg/l}$ ,  $\text{pH}=3.5, t=3\text{ h}$ ,  $T=20\pm 2\text{ }^\circ\text{C}$ , Error < 5%

These represent approx. 14, 96 and 23% zinc, lead and copper removal, respectively. Percentage removals indicate that the adsorption preference for NaP1 is in the order of  $\text{Pb}^{2+} > \text{Cu}^{2+} > \text{Zn}^{2+}$ .

The precipitation/control experiments performed without NaP1, under the same conditions as the adsorption experiments (Fig. 2), showed no reduction in metal concentrations. These demonstrate that the decreases in metal concentrations obtained during the adsorption experiments can only be due to the presence of zeolite NaP1 and not precipitation.

Preliminary multi-cation adsorption experiments were performed at pH 3.5,  $20\pm 2\text{ }^\circ\text{C}$  for 1 h. Figure 3 shows metal uptake of zeolite NaP1 in a multi-cation solution as a function of time and in the absence of precipitation. At pH 3.5, where the concentration of  $\text{H}^+$  ions is  $3.16\times 10^{-4}\text{ M}$  (acidic medium), a low lead uptake (2.1 mg/g) was measured in

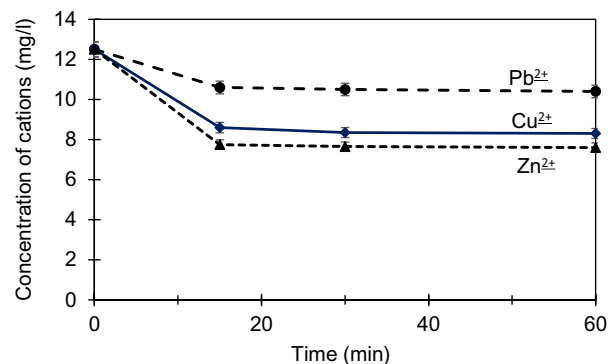


**Fig. 3** Concentrations of heavy metal cations in water as a function of time at pH 3.5 and  $T=20\pm 2\text{ }^\circ\text{C}$  using 1 g/l NaP1 during multi-cation adsorption experiments. Initial metal concentrations were maintained at 12.5 mg/l for each heavy metal

comparison to zinc (4.9 mg/g) and copper (4.2 mg/g). The highest metal uptake at pH 3.5 in multi-cation system was observed for zinc that was the least adsorbed in the single-cation system (6.6 mg/g). In contrast, lead uptake was the highest in the single-cation system (19.2 mg/g) and the least in the multi-cation system. We conducted these experiments with the same initial heavy metal concentrations (12.5 mg/l). Therefore, we eliminated the effect of concentration on the removal.

Adsorptive capacities of adsorbents are generally higher in single cation adsorption compared to multi-cation due to metal competition within the system (Mohan and Singh 2002). There is the possibility of metal/metal competition (Rao et al. 2007) and metal/H<sub>3</sub>O<sup>+</sup> competition at low pH, increasing the positive charge of the zeolite surface, influencing the removal efficiency. Therefore, lead uptake was most influenced by this competition.

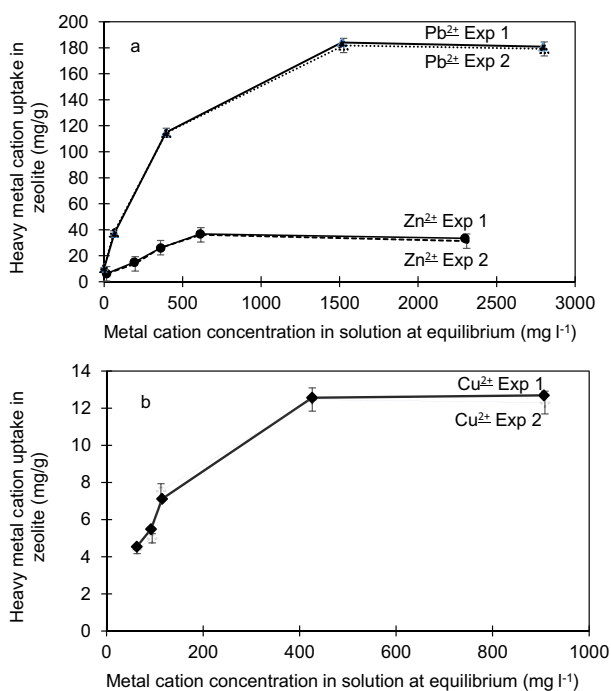


**Fig. 4** Lead and zinc (a) and copper (b) uptakes as a function of equilibrium concentration of cations in water. Conditions: 5 g/l NaP1, Zn<sup>2+</sup> = 50–2300 mg/l, Cu<sup>2+</sup> = 50–1000 mg/l, Pb<sup>2+</sup> = 50–2800 mg/l, pH = 3.5, t = 1 h, T = 20 ± 2 °C. Error < 5%

**Table 3** NaP1 adsorptive capacities of heavy metal cations for Langmuir and Freundlich models

Metal cation	Langmuir			Freundlich		
	Adsorptive capacity (mg/g)	Langmuir constant (b) (l/mg)	R <sup>2</sup>	Adsorptive capacity (mg/g)	Degree of heterogeneity (n)	R <sup>2</sup>
Zinc	34.2	0.0091	0.986	2.41	2.70	0.878
Copper	14.6	0.0077	0.988	0.925	2.48	0.901
Lead	192	0.0064	0.991	21.1	3.72	0.941

Figure 4 shows the amount of heavy metals adsorbed per gram of zeolite over the range of concentrations. An increase in initial concentration of zinc from 50 to 600 mg/l increased the concentration gradient of zinc ions towards available sites, thereby increasing the uptake until the point of saturation, where further increase in zinc concentration (> 600 mg/l) did not change the metal uptake. The shape of the isotherm for zinc closely relates to Type 1 isotherm (Hinze 2001). Therefore, at lower concentrations, more zinc ions can be removed from solution using zeolite NaP1. This is one of the advantages of NaP1 over other adsorbents since most of the current adsorbents and methods are unable to remove metal cations at very low concentrations in large volumes of water (Lakherwal 2014). NaP1 has demonstrated better removal capabilities, in comparison to other adsorbents including activated carbon and clinoptilolite (Koshy and Singh 2016). The heavy metal removal efficiencies for these adsorbents, tested under the similar conditions as NaP1, showed metal removal capacities < 10 mg/g for zinc and copper (Erdem et al. 2004) and < 24 mg/g for lead (Rahman et al. 2016).

The shape of the isotherms are similar to the Langmuir and Type 1 isotherm, as observed for zinc (Fig. 4a, b). However, the lead isotherm is relatively steeper than zinc isotherm, showing a higher affinity of NaP1 to lead than zinc and copper at lower concentrations, demonstrated in similar works for NaP1 (Querol et al. 2002). This implies that lead ions would be removed quicker from solution at lower concentrations, compared to zinc and copper (Hinze 2001).

Data from the adsorption isotherms were evaluated using Langmuir and Freundlich isotherm models to determine the model best fitting the experimental data (Table 3, Figure S3 and S4).

Langmuir model well represented the data for the heavy metal ions since the regression coefficients (R<sup>2</sup>) are in the range of 0.98–0.99. Although Freundlich model was also employed, the regression coefficients were lower than 0.95 (Table 3). Nascimento et al. (2009) used both the Langmuir and Freundlich isotherms in describing the experimental data for NaP1 as the R<sup>2</sup> for both models was above 0.91 for Cu<sup>2+</sup>, Pb<sup>2+</sup> and Zn<sup>2+</sup> metals. However, Alvarez-Ayuso et al. (2003) described their experimental data with Langmuir since R<sup>2</sup> values > 0.99. Similarly, Utami et al. (2019) reported Langmuir isotherm and physisorption (using

Gibbs free energy) for NaP1 derived from natural zeolites. In contrast, Lee et al. (2000) showed better fit with Freundlich model ( $R^2 > 0.82$ ) for NaP1. The maximum adsorption capacity for zinc (34.2 mg/g at pH 3.5) in this study is higher, compared to the other reports in literature (Alvarez-Ayuso et al. 2003) while maximum adsorption capacity for lead (192 mg/g) was similar to Nascimento et al. (2009). In contrast, maximum adsorption capacity for copper (14.6 mg/g) was the lowest, compared to literature, where up to 50–77 mg/g uptakes were reported at pH 4–5 (Alvarez-Ayuso et al. 2003; Nascimento et al. 2009). This is probably due to the source of the fly-ash used for preparation of NaP1, higher pH and concentrations. In contrast, NaP1 adsorbs copper up to five times more than other zeolites such as clinoptilolite (Motsi et al. 2009).

Cation selectivity of an adsorbent can be influenced by several factors including electrostatic forces, ion charge, hydrated radius and precipitate formation (Hendricks 2010). Among these properties, hydrated radius, enthalpy of hydration and sieve action were selected to explain the selectivity zeolite NaP1. Effects of cation charge and complex and precipitate formation were negligible since ions have the same charge and experiments were conducted at pH 3.5, avoiding complex formation and precipitation. The following order for cation selectivity  $Pb^{2+} > Zn^{2+} > Cu^{2+}$  was determined from maximum sorption capacity ( $q_m$ ) (Table 3). However, this does not match the order ( $Pb^{2+} > Cu^{2+} > Zn^{2+}$ ), published in literature for fly-ash derived NaP1 samples (Steenbruggen and Hollman 1998; Lee et al. 2000), clinoptilolite (Sprynskyy et al. 2006), and sodalite (He et al. 2015). The difference may arise from the properties of adsorbent such as Si/Al ratio and experimental conditions, e.g., pH and solid/liquid ratio.

The Langmuir constants (b) for these heavy metals follow the order of  $Zn^{2+} > Cu^{2+} > Pb^{2+}$ . A lower magnitude of Langmuir constant (b) indicates a higher affinity of the adsorbent for the metal. Therefore, results of the Langmuir constant (b) from this study follow the adsorption order of  $Pb^{2+} > Cu^{2+} > Zn^{2+}$ , in line with Steenbruggen and Hollman (1998) and Lee et al. (2000).

Table 4 shows hydrated radius of metals in the order of  $Pb^{2+} < Cu^{2+} < Zn^{2+}$ . A heavy metal ion with a smaller hydrated radius experiences a high electrostatic force of attraction to the surface of the NaP1, explaining the higher metal uptake and affinity of NaP1 for  $Pb^{2+}$  than the other metals. This also implies that less energy is required to attract  $Pb^{2+}$  than  $Cu^{2+}$  and  $Zn^{2+}$ .

Table 4 also shows that the hydrated radius of  $Cu^{2+}$  is smaller than  $Zn^{2+}$ . This suggests that  $Cu^{2+}$  is preferred more than  $Zn^{2+}$ , according to the size of the hydrated radius. However, the experimental results indicate the opposite since the  $Zn^{2+}$  uptake was 2.3 times more than the uptake of  $Cu^{2+}$  ions (Table 3). This may be related to the enthalpy

**Table 4** Comparison of adsorption affinity of NaP1 and properties of heavy metals (Persson 2010)

Metal cation	Hydrated Radius (nm)	Un-hydrated Radius (nm)	Enthalpy of hydration (kJ/mol)	Langmuir constant (b)
Zinc	0.430	0.083	−2050	0.0091
Copper	0.419	0.082	−2100	0.0077
Lead	0.401	0.132	−1480	0.0064

of hydration for these metals, shown in Table 4. During metal uptake from NaP1, hydrated ions may need to lose their water of hydration in order to diffuse through NaP1 pores since their hydrated radii are closer to the pore dimensions (0.31 nm × 0.45 nm) and (0.28 nm × 0.48 nm) of the adsorbent (Alvarez-Ayuso et al. 2003). Enthalpy of hydration represents the affinity of metals to be in solution rather than the solute phase. Hence, a lower value for enthalpy of hydration indicates such cations will lose water and return to the solute phase easier than the others. Therefore,  $Zn^{2+}$  uptake was higher than  $Cu^{2+}$  since  $Zn^{2+}$  can return to the solute phase easier than  $Cu^{2+}$  with the ability to go through the NaP1 micropores. In addition, Table 4 shows  $Pb^{2+}$  with the smallest hydrated radius (0.401 nm) and enthalpy of hydration (−1480 kJ/mol) amongst the heavy metal ions tested ( $Cu = 0.419$  nm,  $Zn = 0.430$  nm) (Persson 2010). When compared to pore dimensions (0.31 nm × 0.45 nm) and (0.28 nm × 0.48 nm) and active pore channel (0.29 nm) of NaP1 (Sharma et al. 2016),  $Pb^{2+}$  is most likely to be preferred to its counterparts. Although the un-hydrated radii of all the elements are below the accessible channels and could get through the zeolite pores, the metals do not exist as single cations in water but are bound to water molecules as hexa-aqua complexes, thus increasing their radii. Therefore, these metals would have to be stripped off the water in order to go through the narrow pores of NaP1 (Erdem et al. 2004). In conclusion, aqueous metal cations exist in water as hydrated ions with radii larger than the pore size of NaP1. The electrostatic forces of attraction between the surface of the zeolite and hydrated cations are influenced by the size of the heavy metals. Thus, smaller hydrated heavy metals are most attracted to the surface of the zeolite. Hence, heavy metals with a low enthalpy of hydration means that they can easily be stripped of water molecules and consequently removed by NaP1. Therefore, in describing the ion selectivity process, regarding the Langmuir sorption capacity,  $Pb^{2+} > Zn^{2+} > Cu^{2+}$  is in line with the study of Hendricks et al. and this is determined by the size of the hydrated cation and its enthalpy of hydration.

The single-cation adsorption data were tested against the pseudo-first and -second order kinetic models to further describe the kinetics of the uptake (Table 5) while the multi-cation adsorption data were only evaluated using

**Table 5** Pseudo-second order kinetic model parameters for heavy metals, obtained from the single and multi-cation adsorption data

Metal cation	Pseudo-second order kinetic model					
	Single-cation adsorption			Multi-cation adsorption		
	$k_2$ (g/mg min)	$Q_e$ (mg/g)	$R^2$	$k_2$ (g/mg min)	$Q_e$ (mg/g)	$R^2$
Lead	6.29	17.7	1	0.00	19.1	1
Copper	21.6	7.20	1	$7.34 \times 10^{-3}$	22.1	1
Zinc	0.061	6.84	0.99	$2.25 \times 10^{-3}$	8.02	0.999

pseudo-second order kinetic model, regarding the results of the data fit for single-cation. The pseudo-second order model best fitted the kinetic data with  $R^2 = 1$  for all three heavy metals, using NaP1. multi-cationmulti-cation.

The pseudo-second order model suggests a heterogenous surface and either a chemisorption or an ion-exchange mechanism, depending on the functional group of the adsorbent. On the other hand, physisorption was proposed using clinoptilolite (Blanchard 1984). Zeolite NaP1 is closely related to clinoptilolite with a similar functional group, thus indicating physisorption as the main metal uptake mechanism. The rate controlling step is possibly particle diffusion through the porous channels of zeolite NaP1 (Erdem et al. 2004; Hendricks 2010). Metal cations are first attracted to the surface of the NaP1 through weak Van der Waal's forces (electrostatic attraction) and diffuse through the pores of NaP1. Diffusion is fast (15 min) but becomes slow (30–180 min) as metals move through the porous structure since the pore dimensions are close to the molecular size of the metals (Erdem et al. 2004).

## Conclusions

Fly-ash derived zeolites could be the possible solution for replacing expensive adsorbents for water and waste-water treatment industry. It is also another solution to utilizing coal fly-ash; waste from the coal power plants being dumped into landfills causing pollution of soil and water bodies. NaP1 displayed fast kinetics with all metals, removing > 80% of the total capacity in 15 min. Metal cation adsorption can be described by the Langmuir isotherm and fitted well to the pseudo-second order kinetic model. Lead removal (96%) was the highest amongst all three metals tested from single cation adsorption experiments. The rate determining step of the uptake mechanism was suggested as the diffusion of metal ions through the pores of NaP1. NaP1 is identified as a crystal structure with heterogenous surface for physical multilayer adsorption of metals while ion selectivity according to Langmuir's constant (b) was in the order of  $Pb^{2+} > Cu^{2+} > Zn^{2+}$ .

**Supplementary Information** The online version contains supplementary material available at <https://doi.org/10.1007/s41742-022-00395-9>.

**Acknowledgements** Frank Ankrah thanks the funding from the Ghana Education Trust Fund (GETFund). The authors thank the Nanoscale and Microscale Centre (nmRC) for providing access to characterisation instruments. Begum Tokay thanks to University of Nottingham, Faculty of Engineering for financial support.

**Author Contributions** AFA—conducted the experiments, interpret the data and discussed and compiled the manuscript. BT—interpret the data, included discussions, edited the manuscript, and supervised the work. CS—contributed the discussions and supervised the work.

**Funding** Ghana Education Trust Fund (GETFund); University of Nottingham, Faculty of Engineering.

**Availability of Data and Material (Data Transparency)** Data will be made available on request.

**Code Availability** Not applicable.

## Declarations

**Conflict of Interest** The authors have no conflicts of interest to declare that are relevant to the content of this article.

**Open Access** This article is licensed under a Creative Commons Attribution 4.0 International License, which permits use, sharing, adaptation, distribution and reproduction in any medium or format, as long as you give appropriate credit to the original author(s) and the source, provide a link to the Creative Commons licence, and indicate if changes were made. The images or other third party material in this article are included in the article's Creative Commons licence, unless indicated otherwise in a credit line to the material. If material is not included in the article's Creative Commons licence and your intended use is not permitted by statutory regulation or exceeds the permitted use, you will need to obtain permission directly from the copyright holder. To view a copy of this licence, visit <http://creativecommons.org/licenses/by/4.0/>.

## References

- Abdullah N, Yusof N, Lau WJ, Jaafar J, Ismail AF (2019) Recent trends of heavy metal removal from water/wastewater by membrane technologies. *J Ind Eng Chem* 76:17–38
- Alvarez-Ayuso E, García-Sánchez A, Querol X (2003) Purification of metal electroplating waste waters using zeolites. *Water Res* 37:4855–4862



- Asim N, Amin MH, Samsudin NA, Badiei M, Razali H, Akhtaruzaman M, Amin N, Sopian K (2020) Development of effective and sustainable adsorbent biomaterial from an agricultural waste material: Cu(II) removal. *Mater Chem Phys* 249:123–128
- Bazrafshan E, Mohammadi L, Ansari-Moghaddam A, Mahvi AH (2015) Heavy metals removal from aqueous environments by electrocoagulation process- a systematic review. *J Environ Health Sci Eng* 13:74
- Blanchard G, Maunay M, Martin G (1984) Removal of heavy metals from waters by means of natural zeolites. *Water Res* 18:1501–1507
- Brännvall E, Kumpiene J (2016) Fly ash in landfill top covers—a review. *Environ Sci Process Impacts* 18:11–21
- Cao D-Q, Wang X, Wang Q-H, Fang X-M, Jin JY, Hao XD, Iritani E, Katagiri N (2020) Removal of heavy metal ions by ultrafiltration with recovery of extracellular polymer substances from excess sludge. *J Membr Sci* 606:118103
- Charentanyarak L (1999) Heavy metals removal by chemical coagulation and precipitation. *Water Sci Technol* 3:135–138
- Czuma N, Baran P, Franus W, Zabierowski P, Zarębska K (2019) Synthesis of zeolites from fly ash with the use of modified two-step hydrothermal method and preliminary SO<sub>2</sub> sorption tests. *SAGE Open* 37:61–76
- Erdem E, Karapinar N, Donat R (2004) The removal of heavy metal cations by natural zeolites. *J Colloid Interface Sci* 280:309–314
- Galletti C, Dosa M, Russo MN, Fino D (2020) Zn<sup>2+</sup> and Cd<sup>2+</sup> removal from wastewater using clinoptilolite as adsorbent. *Environ Sci Pollut Res*. <https://doi.org/10.1007/s11356-020-08483-z>
- He K, Chen Y, Tang Z, Hu Y (2015) Removal of heavy metal ions from aqueous solution by zeolite synthesized from fly ash. *Environ Sci Pollut Res Int* 23:2778–2788
- Hendricks D (2010) Fundamentals of water treatment unit processes: physical, chemical, and biological. CRC Press. <https://doi.org/10.1201/9781439895092>
- Hinz C (2001) Description of sorption data with isotherm equations. *Geoderma* 99:225–243
- Hui KS, Chao CYH, Kot SC (2005) Removal of mixed heavy metal ions in wastewater by zeolite 4A and residual products from recycled coal fly ash. *J Hazard Mater* 127:89–101
- Klučáková M, Pavlíková M (2017) *Lignitic humic* acids as environmentally-friendly adsorbent for heavy metals. *J Chem* 2017:1–5
- Kołodziej D, Krukowska J, Thomas P (2017) Comparison of sorption and desorption studies of heavy metal ions from biochar and commercial active carbon. *Chem Eng J* 307:353–363
- Koshy N, Singh DN (2016) Fly ash zeolites for water treatment applications. *J Environ Chem Eng* 4:1460–1472
- Lakherwal D (2014) Adsorption of heavy metals: a review. *Int J Environ Res Dev* 4:41–48
- Lee M-G, Yi G, Ahn B-J, Roddick F (2000) Conversion of coal fly ash into zeolite and heavy metal removal characteristics of the products. *Korean J Chem Eng* 17:325–331
- Li Y, Bai P, Yan Y, Yan W, Shi W, Xu R (2019) Removal of Zn<sup>2+</sup>, Pb<sup>2+</sup>, Cd<sup>2+</sup>, and Cu<sup>2+</sup> from aqueous solution by synthetic clinoptilolite. *Micropor Mesopor Mater* 273:203–211
- Marchioreto MM, Bruning H, Rulkens W (2005) Heavy metal precipitation in sewage sludge. *Separ Sci Technol* 40:3393–3405
- Margeta K, Logar NZ, Šiljeg M and Farkas A (2013) In: Elshorbagy W and Chowdhury RK (Eds) Natural zeolites in water treatment – How effective is their use. *Water Treatment*. <https://doi.org/10.5772/50738>
- Mohan D, Singh KP (2002) Single- and multi-component adsorption of cadmium and zinc using activated carbon derived from bagasse—an agricultural waste. *Water Res* 36:2304–2318
- Moreno N, Querol X, Ayora C, Pereira CF, Janssen-Jurkovicová M (2001) Utilization of zeolites synthesized from coal fly ash for the purification of acid mine waters. *Environ Sci Technol* 35:3526–3534
- Motsi T, Rowson NA, Simmon MJH (2009) Adsorption of heavy metals from acid mine drainage by natural zeolite. *Int J Miner Process* 92:42–48
- Nascimento M, Soares PSM, Souza VPD (2009) Adsorption of heavy metal cations using coal fly ash modified by hydrothermal method. *Fuel* 88:1714–1719
- Ouki SK, Kavannagh M (1997) Performance of natural zeolites for the treatment of mixed metal-contaminated effluents. *Waste Manag Res* 15:383–394
- Perić J, Trgo M, Medvidović NV (2004) Removal of zinc, copper and lead by natural zeolite—a comparison of adsorption isotherm. *Water Res* 38:1893–1899
- Persson I (2010) Hydrated metal ions in aqueous solution: How regular are their structures? *Pure Appl Chem* 82:1901–1917
- Prasad B, Mortimer R (2011) Treatment of acid mine drainage using fly ash zeolite. *Water Air Soil Pollut* 218:667–679
- Qdais HA, Moussa H (2004) Removal of heavy metals from wastewater by membrane processes: a comparative study. *Desalination* 164:105–110
- Querol X, Umaña JC, Plana F, Alastuey A, Lopez-Soler A, Medinaceli A, Valero A, Domingo MJ, Garcia-Rojo E (2001) Synthesis of zeolites from fly ash at pilot plant scale. *Exempl Potential Appl Fuel* 80:857–865
- Querol X, Moreno N, Umaña JC, Juan R, Hernández S, Fernandez-Pereira C, Ayora C, Janssen M, García-Martínez J, Linares-Solano A, Cazorla-Amoros D (2002) Application of zeolitic material synthesised from fly ash to the decontamination of waste water and flue gas. *J Chem Technol Biotechnol* 77:292–298
- Rahman ML, Sarkar SM, Yusoff MM (2016) Efficient removal of heavy metals from electroplating wastewater using polymer ligands. *Frontiers Environ Sci Eng* 10:352–361
- Ramesh GB, Kumar VR, Muzammil M (2020) Fly ash in concrete using sea water—a review. *Mater Today Proc* 22:890–893
- Ramesh K and Reddy DD (2011) Chapter four: Zeolites and their potential uses in agriculture. In: Sparks DL (ed) *Advances in agronomy*, vol 113. Academic Press, pp 219–241
- Rao GP, Lu C, Su F (2007) Sorption of divalent metal ions from aqueous solution by carbon nanotubes: a review. *Sep Purif Technol* 58:224–231
- Sharma P, Song J-S, Han MH, Cho C-H (2016) GIS-NaP1 zeolite microspheres as potential water adsorption material: Influence of initial silica concentration on adsorptive and physical/topological properties. *Sci Rep* 6:22734
- Sprynskyy M, Buszewski B, Terzyk AP, Namieśnik J (2006) Study of the selection mechanism of heavy metal (Pb<sup>2+</sup>, Cu<sup>2+</sup>, Ni<sup>2+</sup>, and Cd<sup>2+</sup>) adsorption on clinoptilolite. *J Colloid Interface Sci* 304:21–28
- Steenbruggen G, Hollman GGJ (1998) The synthesis of zeolites from fly ash and the properties of the zeolite products. *Geochem Explor* 62:305–309
- Tchounwou PB, Yedjou CG, Patlolla AK, Sutton DJ (2012) Heavy metal toxicity and the environment. *Exp Suppl* 101:133–164
- Timothy N, Williams ET (2019) Environmental pollution by heavy metal: An overview. *Int J Environ Chem* 3:72–82
- Tokay B, Akpinar I (2021) A comparative study of heavy metals removal using agricultural waste biosorbents. *Biores Technol Rep* 15:100719
- Utami AR, Sugiarti S, Sugita P (2019) Synthesis of NaP1 and faujasite zeolite from natural zeolite of ende-ntt as lead (Pb(II)) adsorbent. *Rasayan J Chem* 12:650–658
- Wdowin M, Franus M, Panek R, Badura L, Franus W (2014) The conversion technology of fly ash into zeolites. *Clean Technol Environ Policy* 16:1217–1223

Yan K, Guo Z, Zhao MA, Cheng F (2018) Quantitative analysis of crystalline and amorphous phases in pulverized coal fly ash based on the Rietveld method. *J Non-Cryst Solids* 483:37–42

Zwain HM, Vakili M, Dahlan I (2014) Waste material adsorbents for zinc removal from wastewater: a Comprehensive review. *Int J Chem Eng* 2014:347912